Journal of Non-Newtonian Fluid Mechanics 259 (2018) 16–22

Contents lists available at ScienceDirect

Journal of Non-Newtonian Fluid Mechanics

journal homepage: www.elsevier.com/locate/jnnfm

Axisymmetric Poiseuille flow of a Bingham plastic with rheological parameters varying linearly with pressure

Iasonas Ioannou, Georgios C. Georgiou*

Department of Mathematics and Statistics, University of Cyprus, P.O. Box 20537, Nicosia 1678, Cyprus

ARTICLE INFO

Keywords:
Bingham plastic
Axisymmetric Poiseuille flow
Pressure-dependent viscosity
Pressure-dependent yield stress

ABSTRACT

We consider the steady axisymmetric Poiseuille flow of a Bingham plastic under the assumption that both the plastic viscosity and the yield stress vary linearly with pressure. An analytical solution is derived for the case where the growth coefficients of both rheological parameters are equal, which is indeed a reasonable assumption for certain oil-drilling fluids allowing the existence of a separable solution with a cylindrical unyielded core. The conditions for the occurrence of flow and the effects of the growth coefficient on the radius of the unyielded plug, the velocity profiles and the pressure distributions are discussed.

1. Introduction

Viscoplastic materials, i.e. yield-stress materials, are of great importance in many industrial applications as well as in geophysics, biophysical processes etc [13]. Generally speaking these materials behave as solids below the yield stress, τ_y^*, and as fluid otherwise. It should be noted that throughout the paper starred symbols denote dimensional quantities. The most common constitutive equation describing viscoplasticity is the Bingham-plastic model [2]:

$$\begin{cases} \mathbf{D}^* = \mathbf{0}, & \tau^* \le \tau_y^* \\ \boldsymbol{\tau}^* = 2\left[\dfrac{\tau_y^*}{\dot{\gamma}^*} + \mu^*\right]\mathbf{D}^*, & \tau^* > \tau_y^* \end{cases} \tag{1}$$

where $\boldsymbol{\tau}^*$ is the viscous stress tensor, $\mu^*$is the plastic viscosity, $\mathbf{D}^* \equiv [\nabla^*\mathbf{v}^* + (\nabla^*\mathbf{v}^*)^T]/2$ is the rate of deformation tensor, $\mathbf{v}^*$ is the velocity vector, and $\dot{\gamma}^* \equiv \sqrt{\mathrm{tr}\mathbf{D}^{*2}/2}$ and $\tau^* \equiv \sqrt{\mathrm{tr}\boldsymbol{\tau}^{*2}/2}$ are the magnitudes of $\mathbf{D}^*$ and $\boldsymbol{\tau}^*$, respectively. Setting $\tau_y^* = 0$, Eq. (1) degenerates to the Newtonian constitutive equation. Another popular viscoplastic model is the Herschel–Bulkley model which generalizes the Bingham-plastic model by combining it with the classical power-law constitutive equation [10]. It should be emphasized, however, that these viscoplastic models are idealized. Real-life yield-stress materials exhibit elasto-viscoplastic behavior and thixotropy [5]. In any case, an interesting feature of viscoplastic flows is that the flow domain consists of the so-called unyielded ($\tau^* \le \tau_y^*$) and yielded ($\tau^* > \tau_y^*$) zones where the two branches of the constitutive equation apply. Determining the interface between these regions is not a trivial task, especially in two- and three-dimensional flows [15].

In most isothermal simulations of flows of yield-stress fluids the rheological parameters are assumed to be constant, i.e. independent of pressure. However, this assumption may not be valid in many important applications involving high pressure differences, such as in polymer melt extrusion and injection molding, in tribology, in microfluidics, in geophysical flows, and in oil-drilling and transport ([12,14], and references therein). For example, the viscosity of certain fluids may be a strong function of pressure, while the variation of its density is negligible [4,6].

The pressure-dependence of the yield stress is well established in the mechanics of solid and granular materials [11] and in oil-drilling [9]. The latter authors reported experimental data at different pressures and temperatures for the rheological behavior of two oil-based drilling fluids, obeying the Bingham-plastic and the Herschel–Bulkley models. This data showed that at low temperatures the yield stress decreases linearly with temperature and increases linearly with pressure. In order to model the isothermal yield stress behavior of the two drilling fluids, Hermoso et al. [9] employed the following linear equation

$$\tau_y^*(p^*) = \tau_0^*\left[1 + \beta^*(p^* - p_0^*)\right] \tag{2}$$

where τ_0^* denotes the yield stress at a reference pressure p_0^* and β^* is the yield-stress growth coefficient. As for the plastic viscosity (of the fluid obeying the Bingham plastic equation), Hermoso et al. [9] used the Barus equation

$$\mu^*(p^*) = \mu_0^* e^{\alpha^*(p^* - p_0^*)} \tag{3}$$

where μ_0^* is the plastic viscosity at the reference pressure and $\alpha^* \ge 0$ is the plastic-viscosity growth coefficient [1].

Fusi et al. [7] derived solutions of plane Poiseuille and Couette flows of a Bingham plastic and determined conditions for existence or non-existence of a rigid plug under the assumption that in the yielded region of the flow the velocity is one-dimensional while the pressure is

* Corresponding author.
E-mail address: georgios@ucy.ac.cy (G.C. Georgiou).

https://doi.org/10.1016/j.jnnfm.2018.05.004
Received 19 December 2017; Received in revised form 18 May 2018; Accepted 22 May 2018
Available online 28 May 2018

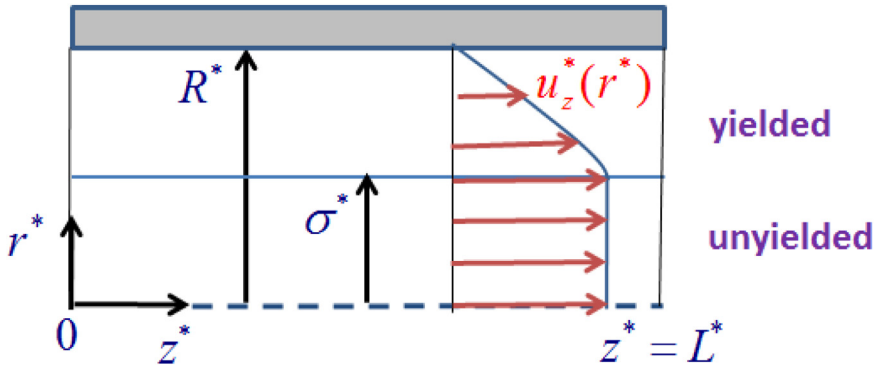

Fig. 1. Geometry of the flow with some symbol definitions and a sketch of the velocity profile.

two-dimensional. Exploiting an integral formulation for the momentum equation in the unyielded part, they derived explicit solutions for the case where the yield stress satisfies the linear Eq. (2) and the plastic viscosity μ^* also varies linearly and vanishes at zero relative pressure, i.e.

$$\mu^*(p^*) = \alpha'^*(p^* - p_0^*) \tag{4}$$

where the constant α'^* has time units. With this assumption, the derivation of an analytical solution becomes easier but the flows of a Bingham plastic with constant rheological parameters or with constant plastic viscosity are not special cases of the flow considered. In other words, the proposed model is not a generalization of the classical Poiseuille flow of a Bingham plastic, describing a rather exotic viscoplastic material whose plastic velocity vanishes at the reference pressure.

In a recent paper, Fusi and Rosso [8] considered the axisymmetric Poiseuille flow of a Herschel–Bulkley fluid assuming that both the consistency index and the yield stress vary linearly with pressure. following equations similar to Eq. (4). In other words, they assumed that the yield stress follows a law of the form

$$\tau_y^*(p^*) = \beta'^*(p^* - p_0^*) \tag{5}$$

where β'^* has time units, an assumption that allows the derivation of explicit solutions. However, with the latter assumptions the standard Herschel–Bulkley solution is not a special case of their model. Moreover, because Eqs. (4) and (5) are realistic only at high values of the pressure, the central plug region is suppressed considerably. In most plots presented by Fusi and Rosso [8] the solutions are almost fully-yielded and very similar to their power-law counterparts.

Damianou and Georgiou [3] analyzed the plane Poiseuille flow of a Bingham plastic with pressure-dependent material parameters assuming that the yield stress and the plastic viscosity obey respectively Eq. (2) and the linear law

$$\mu^*(p^*) = \mu_0^*\left[1 + \alpha^*(p^* - p_0^*)\right] \tag{6}$$

which can be viewed as the linearization of Eq. (3) for low values of α^* and low pressures. Under these assumptions, the tensorial form of the constitutive equation becomes:

$$\begin{cases} \mathbf{D}^* = \mathbf{0}, & \tau^* \le \tau_y^*(p^*) \\ \boldsymbol{\tau}^* = 2\left[\dfrac{\tau_0^*\left[1 + \beta^*(p^* - p_0^*)\right]}{\dot{\gamma}^*} + \mu_0^*\left[1 + \alpha^*(p^* - p_0^*)\right]\right]\mathbf{D}^*, & \tau^* > \tau_y^*(p^*) \end{cases} \tag{7}$$

When $\alpha^* = \beta^* = 0$, Eq. (7) is reduced to the classical Bingham plastic constitutive equation with constant material parameters. Damianou and Georgiou [3] reported explicit solutions for the velocity, the pressure, and the height of the central unyielded region, which are generalizations of the solutions for a Bingham plastic with constant rheological parameters or with constant plastic viscosity and are valid equally at low and high pressures. It should be noted that Eq. (6) can be used safely only in processes where the pressure difference $(p^* - p_0^*)$ is such that the plastic viscosity remains positive, e.g. in Poiseuille flows. Otherwise, the Barus Eq. (3) is a safer choice.

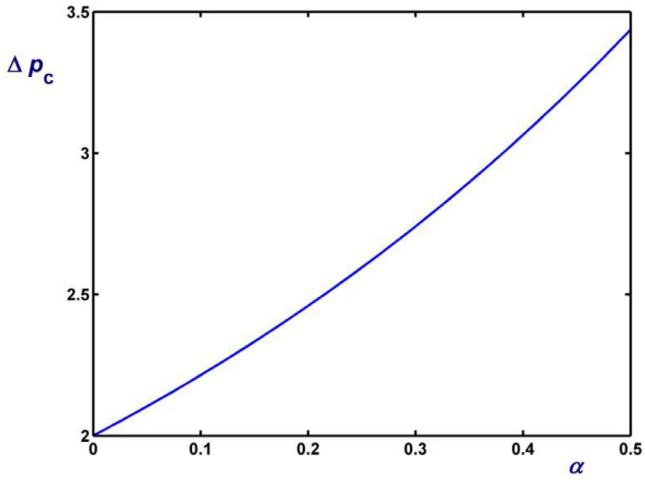

Fig. 2. Variation of the critical pressure difference $\Delta p_c \equiv \Delta p_c^*/(\tau_0^* L^*/R^*)$ required for the initiation of Bingham-plastic flow with the growth parameter α.

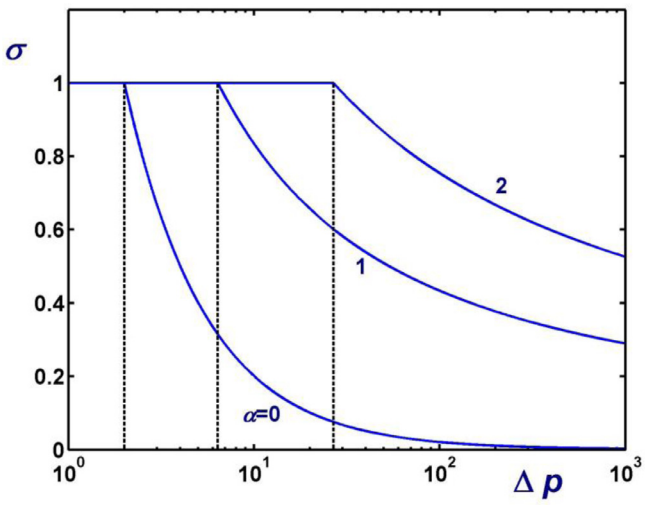

Fig. 3. Radius of the unyielded core for various values of the growth parameter α. The vertical lines indicate the critical pressure required for flow to occur.

In a subsequent work, Panaseti et al. [14], extending a method proposed by Fusi et al. [7], modeled the lubrication flow of a Herschel–

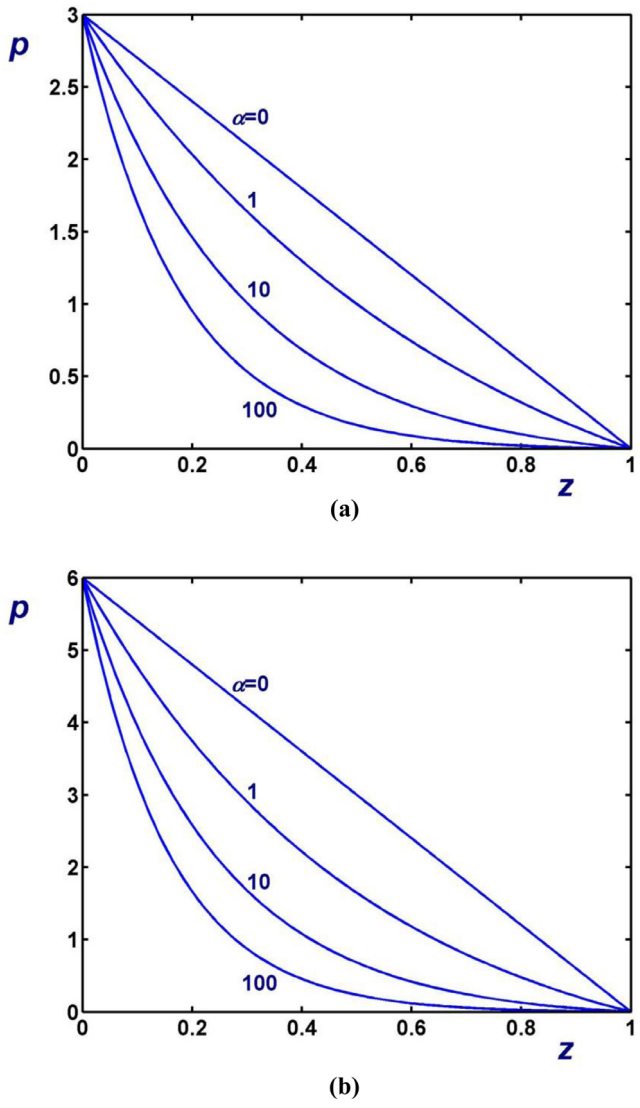

Fig. 4. Dimensionless pressure in the unyielded core (where the pressure is one-dimensional): (a) $\Delta p = 3$; (b) $\Delta p = 6$.

Bulkley fluid in a symmetric long channel of varying width, assuming again that both the consistency index and the yield stress vary linearly with pressure. Under the lubrication approximation the shape of the yield surface depends only on the shape of the wall and the power-law exponent, while its elevation depends on all parameters. Thus, the width of the unyielded core in a channel of constant width is also constant, despite the pressure dependence of the yield stress. Panaseti et al. [14] also derived semi-analytical results for the case of a channel of linearly decreasing width and numerical results for non-linear wall functions.

The objective of the present work is to study the axisymmetric Poiseuille flow of a Bingham plastic with material parameters varying linearly with pressure following Eqs. (2) and (6). As shown below, unlike its planar counterpart, the axisymmetric flow is amenable to an analytical unidirectional solution only in the special case that $\alpha^* = \beta^*$. Such a solution is still of interest, given that the two parameters are very similar for certain oil-drilling fluids, e.g. for fluid B34 studied by Hermoso et al. [9], as discussed in the Appendix.

In Section 2, the governing equations for the axisymmetric Poiseuille flow of a Bingham plastic with pressure-dependent material parameters are presented. In Section 3, the analytical solution when $\alpha^* = \beta^*$ is derived. This is discussed in Section 4. The conclusions of this work are summarized in Section 5.

2. Governing equations

Consider now the axisymmetric Poiseuille flow, of a material obeying Eq. (7), in a horizontal tube of constant circular cross section, with radius R^* and length L^*, as illustrated in Fig. 1. Working with cylindrical coordinates, the z- and r-axes are taken in the main-flow and transverse directions, respectively. With the assumption that the flow is unidirectional with $v_z^* = v_z^*(r^*)$ and $v_r^* = 0$, the unyielded core is cylindrical of radius $r^* = \sigma^*$, where $0 < \sigma^* < R^*$, and the continuity equation is automatically satisfied.

In the yielded region, i.e. $(z^*, r^*) \in [0, L^*] \times [\sigma^*, R^*]$, the pressure is two-dimensional, i.e. $p^* = p^*(z^*, r^*)$ and the only non-zero component of the stress tensor is the shear stress:

$$\tau_{rz}^* = -\tau_0^* \left[1 + \beta^*(p^* - p_0^*)\right] + \mu_0^* \left[1 + \alpha^*(p^* - p_0^*)\right] \frac{dv_z^*}{dr^*} \tag{8}$$

The z- and r-components of the momentum equation read:

$$-\frac{\partial p^*}{\partial z^*} + \frac{1}{r^*}\frac{\partial (r^* \tau_{rz}^*)}{\partial r^*} = 0 \tag{9}$$

and

$$-\frac{\partial p^*}{\partial r^*} + \frac{\partial \tau_{rz}^*}{\partial z^*} = 0 \tag{10}$$

respectively. On the pipe wall, the usual no-slip condition is assumed, i.e. $v_z^*(R^*) = 0$, and at the yield surface, the velocity is given by $v_z^*(\sigma^*) = v_c^*$, where v_c^* is the velocity of the plug core.

In the unyielded region, i.e. for $(z^*, r^*) \in [0, L^*] \times [0, \sigma^*]$, the velocity is constant, $v_z^* = v_c^*$, and the pressure is one-dimensional, $p^* = p^*(z^*)$, with the assumption that

$$p^*(0) = p_i^* \quad \text{and} \quad p^*(L^*) = p_0^* \tag{11}$$

For steady-state flow in the absence of body forces, the integral balance of linear momentum in the unyielded region is exploited, as suggested by Fusi and Rosso [8]:

$$2\int_0^{L^*} \tau_{rz}^*\big|_{r^*=\sigma^*} dz^* + \sigma^*(p_i^* - p_0^*) = 0 \tag{12}$$

Given that at the yield surface ($r^* = \sigma^*$) the velocity derivative vanishes, from Eqs. (8) and (12) one finds that

$$\sigma^* = 2\left[1 + \frac{\beta^*}{L^*}\int_0^{L^*} (p^* - p_0^*)_{r^*=\sigma^*} dz^*\right]\frac{\tau_0^* L^*}{\Delta p^*} \tag{13}$$

where $\Delta p^* = p_i^* - p_0^*$. The use of Eq. (12) is critical, since, as pointed out by Fusi and Rosso [8], the classical differential momentum equation cannot be used in the unyielded domain, where the viscoplastic stress is not defined.

2.1. Non-dimensionalisation

The problem is dedimensionalised by scaling z^* by L^*, r^* and σ^* by R^*, $(p^* - p_o^*)$ by τ_0^*/ε, v_z^* by $\tau_0^* R^*/\mu_0^*$, and the stress components by τ_o^*, where $\varepsilon \equiv R^*/L^*$ is the tube aspect ratio. Therefore, the dimensionless form of Eq. (13) becomes

$$\sigma = \frac{2}{\Delta p}\left[1 + \beta\int_0^1 p|_{r=\sigma} dz\right] \tag{14}$$

where $\Delta p \equiv \Delta p^*/(\tau_0^*/\varepsilon)$ is the dimensionless pressure drop along the channel and $\beta \equiv \beta^* \tau_0^*/\varepsilon$. Thus, in the yielded region, i.e. for $(z, r) \in [0, 1] \times [\sigma, 1]$, the dimensionless shear stress is given by

$$\tau_{rz} = -(1 + \beta p) + (1 + \alpha p)\frac{dv_z}{dr} \tag{15}$$

where $\alpha \equiv \alpha^* \tau_0^*/\varepsilon$, and the two components of the momentum equation read:

$$-\frac{\partial p}{\partial z} + \frac{1}{r}\frac{\partial (r\tau_{rz})}{\partial r} = 0 \tag{16}$$

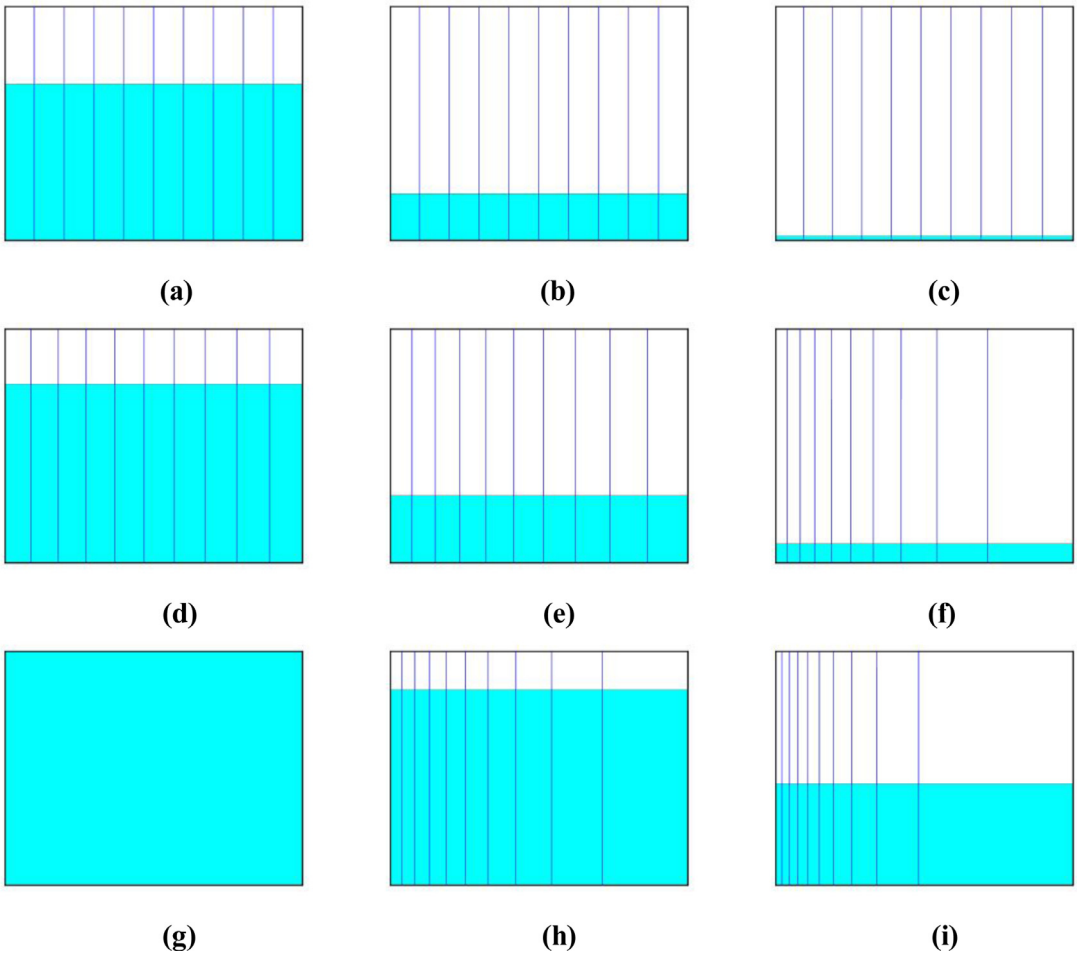

Fig. 5. Effect of the growth parameter α on the pressure contours for $\varepsilon = 0.01$: (a) $\alpha = 0$, $\Delta p = 3$; (b) $\alpha = 0$, $\Delta p = 10$; (c) $\alpha = 0$, $\Delta p = 100$; (d) $\alpha = 0.1$, $\Delta p = 3$; (e) $\alpha = 0.1$, $\Delta p = 10$; (f) $\alpha = 0.1$, $\Delta p = 100$; (g) $\alpha = 1$, $\Delta p = 3$; (h) $\alpha = 1$, $\Delta p = 10$; (i) $\alpha = 1$, $\Delta p = 100$.

and

$$-\frac{\partial p}{\partial r} + \varepsilon^2 \frac{\partial \tau_{rz}}{\partial z} = 0 \tag{17}$$

Substituting Eq. (15) into Eqs. (16) and (17) we get

$$\frac{\partial p}{\partial z} = \left(\alpha \frac{dv_z}{dr} - \beta\right)\frac{\partial p}{\partial r} + (1+\alpha p)\frac{d^2 v_z}{dr^2} - \frac{1+\beta p - (1+ap)\frac{dv_z}{dr}}{r} \tag{18}$$

and

$$\frac{\partial p}{\partial r} = \varepsilon^2\left(\alpha \frac{dv_z}{dr} - \beta\right)\frac{\partial p}{\partial z} \tag{19}$$

Substituting Eq. (19) into Eq. (18) and moving terms involving the velocity to the RHS, one gets:

$$\frac{\partial p/\partial z}{1+\alpha p} = \frac{d^2 v_z/dr^2 + (1/r)dv_z/dr}{1-\varepsilon^2\left(\alpha dv_z/dr - \beta\right)^2} - \frac{1/r}{1-\varepsilon^2\left(\alpha dv_z/dr - \beta\right)^2}\frac{1+\beta p}{1+\alpha p} \tag{20}$$

It is readily observed that variables can be separated and an analytical solution can be obtained only in the special case where $a = \beta$. This solution is derived below.

3. Analytical solution for $\alpha = \beta$

When $a = \beta$, Eq. (20) is simplified as follows:

$$\frac{\partial p/\partial z}{1+\alpha p} = \frac{d^2 v_z/dr^2 + (1/r)dv_z/dr - 1/r}{1-\varepsilon^2\alpha^2\left(dv_z/dr - 1\right)^2} = -\Lambda \tag{21}$$

where Λ is a positive constant to be determined; given that the pressure is expected to be a strictly decreasing function of the axial distance, the RHS of Eq. (21) has been chosen to have a minus sign. Thus, in the yielded region, we have two differential equations to be solved for v_z and p. Solving the one for v_z and applying the boundary conditions $dv_z/dr(r=\sigma) = v_z(r=1) = 0$, we get (for $\alpha > 0$):

$$v_z(r) = -\frac{1}{\varepsilon^2\alpha^2\Lambda}\ln\frac{\left[I_o(\varepsilon a\Lambda r) + cK_o(\varepsilon a\Lambda r)\right]}{\left[I_o(\varepsilon a\Lambda) + cK_o(\varepsilon a\Lambda)\right]} - (1-r), \quad \sigma \le r \le 1 \tag{22}$$

where I_o and K_o are the modified Bessel functions of first and second kind, respectively, and

$$c = \frac{I_1(\varepsilon a\Lambda\sigma) - \varepsilon a I_o(\varepsilon a\Lambda\sigma)}{K_1(\varepsilon a\Lambda\sigma) + \varepsilon a K_o(\varepsilon a\Lambda\sigma)} \tag{23}$$

Integrating now the differential equation for the pressure in Eq. (21) yields

$$p(z,r) = \frac{1}{\alpha}\left[w(r)e^{-\alpha\Lambda z} - 1\right], \quad \sigma \le r \le 1 \tag{24}$$

where $w(r)$ is an unknown function. Substituting p and v_z into Eq. (19), we get a first-order differential equation for w,

$$w'(r) - \varepsilon\alpha\Lambda\frac{\left[I_1(\varepsilon a\Lambda r) - cK_1(\varepsilon a\Lambda r)\right]}{\left[I_o(\varepsilon a\Lambda r) + cK_o(\varepsilon a\Lambda r)\right]}w(r) = 0 \tag{25}$$

the solution of which is

$$w(r) = C\left[I_o(\varepsilon a\Lambda r) + cK_o(\varepsilon a\Lambda r)\right] \tag{26}$$

where C is an integration constant. Applying the conditions $p(0,\sigma) = \Delta p$ and $p(1,\sigma) = 0$ leads to

$$C = \frac{1+\alpha\Delta p}{I_o(\varepsilon a\Lambda\sigma) + cK_o(\varepsilon a\Lambda\sigma)} \quad \text{and} \quad \Lambda = \frac{\ln(1+\alpha\Delta p)}{\alpha} \tag{27}$$

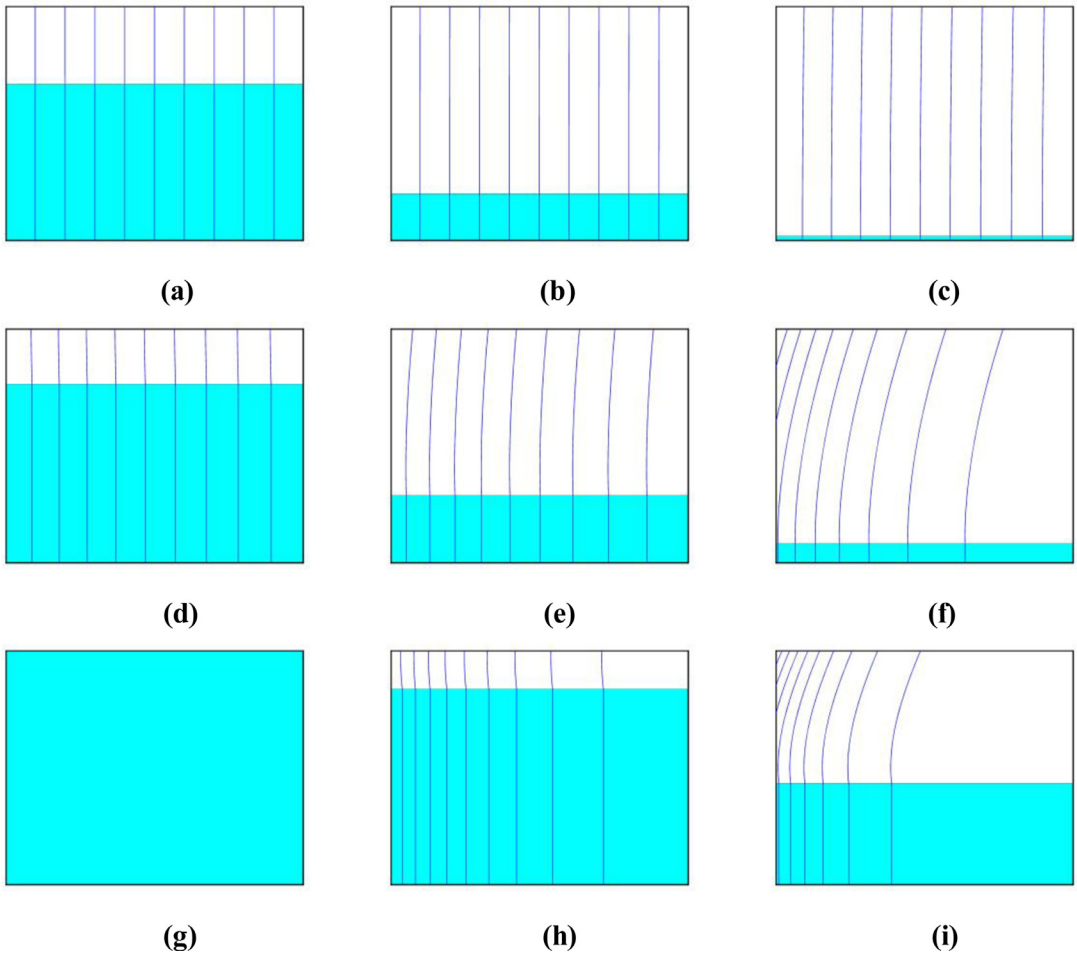

Fig. 6. Effect of the growth parameter α on the pressure contours for $\varepsilon = 0.5$: (a) $\alpha = 0$, $\Delta p = 3$; (b) $\alpha = 0$, $\Delta p = 10$; (c) $\alpha = 0$, $\Delta p = 100$; (d) $\alpha = 0.1$, $\Delta p = 3$; (e) $\alpha = 0.1$, $\Delta p = 10$; (f) $\alpha = 0.1$, $\Delta p = 100$; (g) $\alpha = 1$, 3; (h) $\alpha = 1$, $\Delta p = 10$; (i) $\alpha = 1$, $\Delta p = 100$. The high value of ε was chosen in order to exaggerate the differences.

Therefore, we have:

$$p(z,r) = \begin{cases} \frac{1}{\alpha}\left[(1+\alpha\Delta p)^{1-z}\dfrac{I_o(\varepsilon a\Lambda r)+cK_o(\varepsilon a\Lambda r)}{I_o(\varepsilon a\Lambda\sigma)+cK_o(\varepsilon a\Lambda\sigma)}-1\right], & \sigma \le r \le 1 \\ \frac{1}{\alpha}\left[(1+\alpha\Delta p)^{1-z}-1\right], & 0 \le r < \sigma \end{cases} \tag{28}$$

By means of Eq. (14), the yield point is given by

$$\sigma = \frac{2\alpha}{\ln(1+\alpha\Delta p)} \tag{29}$$

and thus $\Lambda\sigma = 2$. Therefore, expression (23) for the constant c becomes:

$$c = \frac{I_1(2\varepsilon a) - \varepsilon a I_o(2\varepsilon a)}{K_1(2\varepsilon a) + \varepsilon a K_o(2\varepsilon a)} \tag{30}$$

As for the velocity, one finds

$$v_z(r) = \begin{cases} -\frac{\sigma}{2\varepsilon^2\alpha^2}\ln\dfrac{\left[I_o(2\varepsilon ar/\sigma)+cK_o(2\varepsilon ar/\sigma)\right]}{\left[I_o(2\varepsilon a/\sigma)+cK_o(2\varepsilon a/\sigma)\right]}-(1-r), & \sigma \le r \le 1 \\ -\frac{\sigma}{2\varepsilon^2\alpha^2}\ln\dfrac{\left[I_o(2\varepsilon a)+cK_o(2\varepsilon a)\right]}{\left[I_o(2\varepsilon a/\sigma)+cK_o(2\varepsilon a/\sigma)\right]}-(1-\sigma), & 0 \le r < \sigma \end{cases} \tag{31}$$

When $a = \beta = 0$, $\sigma = 2/\Delta p$ and the velocity and the pressure are respectively given by

$$v_z(r) = \begin{cases} \frac{\Delta p}{4}\left(1-r^2\right)-(1-r), & \sigma \le r \le 1 \\ \frac{\Delta p}{4}\left(1-\sigma^2\right)-(1-\sigma), & 0 \le r < \sigma \end{cases} \tag{32}$$

and

$$p(z) = \Delta p\,(1-z) \tag{33}$$

4. Discussion

The critical pressure difference required to start the flow is of importance in engineering applications. This can be found from Eq. (29) as the pressure difference at which $\sigma = 1$:

$$\Delta p_c = \frac{e^{2\alpha}-1}{\alpha} \tag{34}$$

For the case $\alpha = 0$ (pressure-independent rheological parameters), $\Delta p_c = 2$. The effect of the growth number α on the critical pressure difference needed for flow to occur is illustrated in Fig. 2. As expected, Δp_c increases rapidly with α. The variation of the unyielded core radius σ with the pressure difference Δp is illustrated in Fig. 3 for $\alpha = 0$, 1, and 2. Below the critical pressure difference Δp_c, σ is equal to 1 (since there is no flow) and then it decreases with Δp. The rate of this decrease is reduced as α is increased.

As already mentioned, the pressure in the unyielded core is one-dimensional, given by

$$p(r \le \sigma, z) = \begin{cases} \frac{1}{\alpha}\left[(1+\alpha\Delta p)^{1-z}-1\right], & \alpha > 0 \\ (1-z)\Delta p, & \alpha = 0 \end{cases} \tag{35}$$

Fig. 4 shows the pressure distributions in the unyielded core for $\Delta p = 3$ and 6 and different values of α ranging from 0 to the extreme value of 100. As the growth number α increases, the pressure deviates from the linear distribution corresponding to $\alpha = 0$, so that the pressure gradient increases near the inlet plane where the plastic viscosity and the yield stress attain their maximum values and decreases near the exit where both parameters are minimum.

In the yielded region, the pressure is two-dimensional. The effects of the growth parameter α and the imposed pressure difference Δp on the pressure contours as well as on the radius of the plug are illustrated in Figs. 5 and 6 for $\varepsilon = 0.01$ and 0.5, respectively. When the aspect ratio ε is low (which is the case in applications), the pressure in the yielded region remains essentially one dimensional; as a result, the contours are vertical straight lines. The contours are equidistant only when $\alpha = 0$. Otherwise, the distance between the contours increases downstream and this effect is more pronounced as both α and Δp are increased. The two-dimensional character of the flow is exaggerated in Fig. 6, where the rather high value $\varepsilon = 0.5$ for the aspect ratio has intentionally been chosen.

Fig. 7 shows velocity profiles for $\alpha = 0$ (pressure-independent material parameters), 1 and 2 and different values of the imposed pressure difference. The corresponding critical pressure differences are 2, $(e^2 - 1)$ and $(e^4 - 1)/2$. As expected, the velocity is reduced as α is increased.

Finally, in Fig. 8, the (dimensionless) volumetric flow rate, defined by

$$Q \equiv 2\int_0^1 v_z(r) r dr \tag{36}$$

is plotted versus the imposed pressure difference Δp for $\varepsilon = 0.01$ and four different values of α (0, 0.001, 0.01, and 0.1). The variation of Q with Δp is linear only when $\alpha = 0$, i.e. the rate of increase is constant. As α is increased, this rate becomes more dependent on Δp, decreasing with both α and Δp. It should be noted that the volumetric flow rate below $\Delta p_c = (e^{2\alpha} - 1)/\alpha$ is zero; as a result, the curves of Fig. 8 do not start from the origin.

Comparing the present results with those of Fusi and Rosso [8], we may briefly note the following: (a) the model of Fusi and Rosso [8] allows the solution of Herschel–Bulkley flow with different linear variations of the consistency index and the yield stress, which however are not reduced to the classical constant-parameter solutions; (b) both models predict that the curvature of the pressure contours increases as the imposed pressure difference increases; (c) both models predict an unyielded core region of constant radius. With the model of Fusi and Rosso [8], σ depends on the yield-stress growth coefficient and not on the consistency-index growth coefficient (which are equal in the present work). This is also the case for the pressure distribution. Interestingly, in the case of plane Poiseuille flow with the yield stress and the plastic viscosity following Eqs. (2) and (6), respectively, the semi-width σ of the unyielded region depends on both α and β [3].

5. Conclusions

We have analysed the fully-developed axisymmetric Poiseuille flow of a Bingham plastic assuming that the yield stress and the plastic viscosity vary linearly with pressure and derived an analytical solution for the case where the growth coefficients for both rheological parameters are equal. The latter assumption, which is valid for certain drilling fluids, allows the existence of a separable solution with a cylindrical unyielded core. The critical pressure difference required for the initiation of flow increases exponentially with the common growth coefficient. The effects of that coefficient on the pressure distributions and the velocity profiles have been investigated.

In our current research efforts, we study the general flow where the growth coefficients of the plastic viscosity and the yield stress are not equal, $\alpha^* \neq \beta^*$, considering both semi-analytical solutions for simplified cases and numerical solutions of the general axisymmetric flow of a Bingham plastic with pressure-dependent rheological parameters. It is clear that in the general case, the flow is fully two-dimensional and σ is not constant, which implies that the unyielded core may be converging or diverging, depending on the relative values of α^* and β^*.

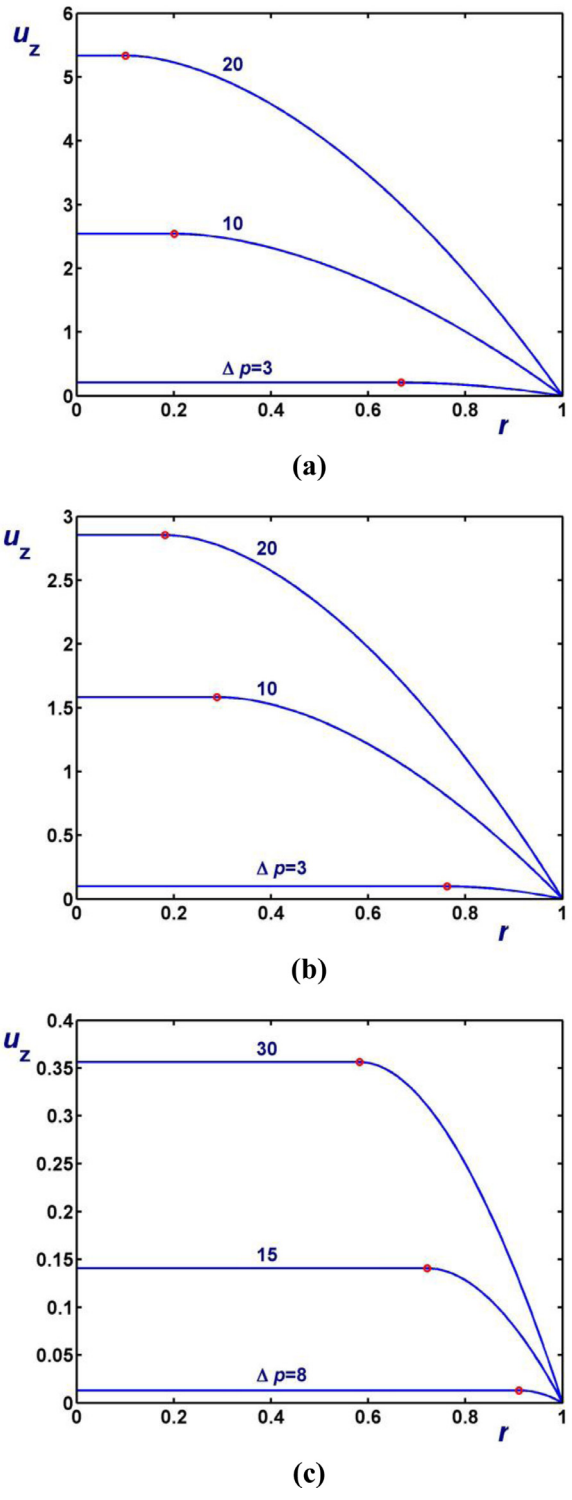

Fig. 7. Velocity distributions of Bingham plastic flow for $\varepsilon = 0.01$ and different values of the imposed pressure difference: (a) $\alpha = 0$ (constant material parameters); (b) $\alpha = 0.1$; (c) $\alpha = 1$. The circles show the positions of the yield point.

Appendix: estimates of the plastic-viscosity and yield-stress growth parameters

Hermoso et al. [9] investigated experimentally the effects of temperature and pressure on the values of the rheological parameters of two oil-based drilling fluids. The values of the plastic viscosity, μ^*, and of the yield stress, τ_y^*, for the first fluid (B34 fluid), which was found to follow

Table 1
Data of Hermoso et al. [9]) for the B34-based drilling fluid at different temperatures and pressures and the calculated growth coefficients.

ΔP (bar)	0		200		390		Calculated material constants			
T (°C)	μ_0^* (Pa s)	τ_0^* (Pa)	μ^* (Pa s)	τ_y^* (Pa)	μ^* (Pa s)	τ_y^* (Pa)	μ_o (Pa s)	τ_o (Pa)	α^* (Pa^{-1})	β^* (Pa^{-1})
40	0.164	0.16	0.301	0.41	0.502	0.74	0.152	0.144	5.68E-08	1.02E-7
80	0.03	0.07	0.043	0.11	0.063	0.2	0.028	0.061	2.93E-08	5.41E-8
100	0.017	0.08	0.023	0.11	0.028	0.17	0.017	0.075	1.65E-08	3.08E-8
120	0.012	0.01	0.014	0.12	0.02	0.15	0.011	0.022	1.80E-08	1.61E-8
140	0.009	0.14	0.017	0.18	0.019	0.21	0.01	0.141	2.59E-08	1.27E-8

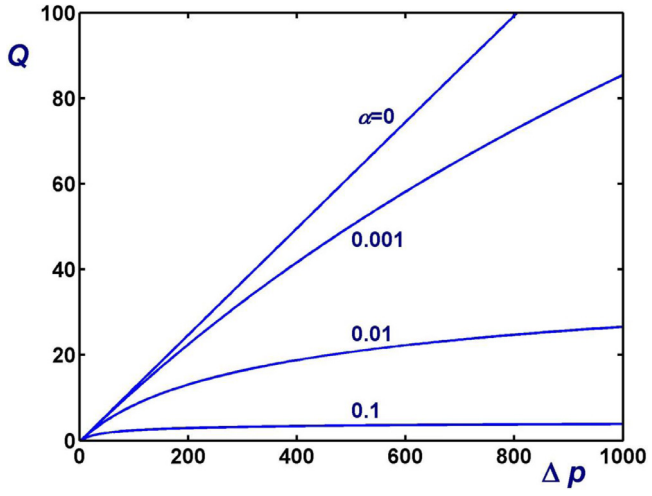

Fig. 8. The volumetric flow rate as a function of the imposed pressure difference for various values of the growth parameter α and $\epsilon = 0.01$.

the Bingham-plastic constitutive equations, are tabulated in Table 1. In the range of their experiments both the plastic viscosity and the yield stress increase with pressure and decrease with temperature, at least at low temperatures. Around 120–140 °C a sudden increase in the values of the two parameters is observed. In the last two columns of Table 1, we list the values of the two growth parameters α^* and β^* obtained at each temperature using least squares. It can be seen that the two parameters are of the same order and that β^* is greater than α^* only at low temperatures and that the opposite is true at 120 °C. Hence, assuming that the two parameters are equal is a reasonable assumption.

References

[1] C. Barus, Isothermals, isopiestics and isometrics relative to viscosity, Am. J. Sci. 45 (1893) 87–96.
[2] EC Bingham, Fluidity and Plasticity, McGraw Hill, New-York, 1922.
[3] Y. Damianou, G.C. Georgiou, On Poiseuille flows of a Bingham plastic with pressure-dependent rheological parameters, J. Non-Newtonian Fluid Mech. 250 (2017) 1–7.
[4] M.M. Denn, Polymer Melt Processing, Cambridge University Press, Cambridge, 2008.
[5] R.H. Ewoldt, G.H. McKinley, Mapping thixo-elasto-visco-plastic behavior, Rheol. Acta 56 (2017) 195–210.
[6] L. Fusi, A. Farina, F. Rosso, Bingham flows with pressure-dependent rheological parameters, Int. J. Nonlinear Mech. 64 (2014) 33–38.
[7] L. Fusi, A. Farina, F. Ross, S. Roscani, Pressure-driven lubrication flow of a Bingham fluid in a channel: a novel approach, J. Non-Newtonian Fluid Mech. 221 (2015) 66–75.
[8] L. Fusi, F. Rosso, Creeping flow of a Herschel–Bulkley fluid with pressure-dependent material moduli, Eur. J. Appl. Math.. doi.10.1017/S0956792517000183
[9] J. Hermoso, F. Martinez-Boza, C. Gallegos, Combined effect of pressure and temperature on the viscous behaviour of all-oil drilling fluids, Oil Gas Sci. Technol. Rev. IFP Energies Nouvelles 69 (2014) 1283–1296.
[10] W. Herschel, R. Bulkley, Measurement of consistency as applied to rubber-benzene solutions, Proc. Am. Soc. Test Mater. 26 (1926) 621–633.
[11] I.R. Ionescu, A. Mangeney, F. Bouchut, O. Roche, Viscoplastic modeling of granular column collapse with pressure-dependent rheology, J. Non-Newtonian Fluid Mech. 219 (2015) 1–18.
[12] J. Málek, K.R. Rajagopal, Mathematical properties of the solutions to the equations governing the flow of fluids with pressure and shear rate dependent viscosities, Handbook of Mathematical Fluid Dynamics, Elsevier, 2007.
[13] A. Malkin, V. Kulichikhin, S. Ilyin, A modern look on yield stress fluids, Rheol. Acta 56 (2017) 177–188.
[14] P. Panaseti, Y. Damianou, G.C. Georgiou, K.D. Housiadas, Pressure-driven flow of a Herschel–Bulkley fluid with pressure-dependent rheological parameters, Phys. Fluids 30 (2018) 030701.
[15] P. Saramito, A. Wachs, Progress in numerical simulation of yield stress fluid flows, Rheol. Acta 56 (2017) 211–230.